Journal of Alloys and Compounds 546 (2013) 41–47

Contents lists available at SciVerse ScienceDirect

Journal of Alloys and Compounds

journal homepage: www.elsevier.com/locate/jalcom

Effect of vanadium substitution for zirconium on the glass forming ability and mechanical properties of a $Zr_{65}Cu_{17.5}Ni_{10}Al_{7.5}$ bulk metallic glass

Nima Khademian [a,*], Reza Gholamipour [b], Farzad Shahri [c], Morteza Tamizifar [c]

[a] Department of Mechanics, Islamshahr Branch, Islamic Azad University (IAU), Tehran, Iran
[b] Iranian Research Organization for Science and Technology (IROST), Tehran, Iran
[c] Faculty of Engineering and High-Tech., Iran University of Industries and Mines (IUIM), Tehran, Iran

ARTICLE INFO

Article history:
Received 21 June 2012
Received in revised form 6 August 2012
Accepted 8 August 2012
Available online 17 August 2012

Keywords:
Bulk metallic glass
Compression strength
Fracture surface
Shear bands
Vanadium substitution

ABSTRACT

Effect of vanadium on the thermal and mechanical properties of the $Zr_{65}Cu_{17.5}Ni_{10}Al_{7.5}$ bulk metallic glass has been studied. The vanadium substitution for zirconium in the bulk metallic glass leads to the decrease of the glass forming ability in constant cooling rate; as well as co-precipitation of Zr_2Ni and Zr_2Cu crystalline phases in amorphous matrix. The size of the crystallites are about 20–50 nm in amorphous matrix and they act as a barrier against of rapid propagation of shear bands. In fact, the nanocrystalline phases in amorphous matrix cause the increase of the strain and the quasi-static compression strength about 58% and 20%, respectively.

1. Introduction

Bulk metallic glasses as relatively new materials are the most commonly candidates for structural applications, during the last two decades. These innovative materials open up unlimited possibilities for modern material science and development. Depend on the application; the characteristics of BMGs can be designed into a custom-made material. The properties of these new materials are basically determined by the properties of their components. The development objectives for BMGs are: an improvement in wear resistance, enhanced resistance to corrosion, high strength and large elastic limit, on the other hand, limited plasticity (0–2% plastic strain) prior to failure which constrains their applications as structural materials [1–8].

Zr-based bulk glassy alloys have attracted widespread interests because of their strong glass forming ability and wide supercooled liquid regions; however many studies are still focused on the development of new alloy compositions due to their attractive properties and technological applications [9–19].

In order to improve the ductility, heterogeneous microstructures have recently been designed by combining glassy matrix with crystalline second phase. The second phase in metallic glasses can be introduced by partial crystallization of the metallic glass, especially during the solidification. The precipitation of crystalline phase in the glassy matrix may be induced by the addition of elements which cause partial crystallization during solidification [10,16–18,20].

This paper intends to present the effect of the substitution of a small amount of V for Zr on thermal and mechanical properties of $Zr_{65-x}Cu_{17.5}Ni_{10}Al_{7.5}V_x$ (x = 0, 1, 2, 3, 5) bulk metallic glass. We report correlations among the elastic moduli, fracture strength, Vicker's hardness and glass transition for bulk metallic glasses. The clear correlations imply that the mechanical properties of BMGs would be better controlled by selection of elements and quantity of them.

2. Experimental

Zr-based alloy ingots with composition of $Zr_{65-x}Cu_{17.5}Ni_{10}Al_{7.5}V_x$ (x = 0, 1, 2, 3, 5) prepared by arc melting using high purity elements in Ti-gettered Ar atmosphere on a water cooled copper crucible. Cylindrical rod alloys of about 30 mm in length and 4 mm in diameter were produced by a suction casting method. The structure of the samples was examined preliminarily by X-ray diffraction (XRD) using an X'Pert XRD-Philips diffractometer with Co-K_α radiation (λ = 0.178 nm). Thermal analysis was carried out by differential scanning calorimetry (DSC) with heating rate of 20 K/min by a NETZSCH 449 DSC. Compressive tests were performed at the strain rate of 10^{-4} s^{-1} by an INSTRON machine. Specimens for compression test with dimensions of 4 mm in diameter and 8 mm in height were machined from the suction casting samples. Fracture surfaces of compression tested samples were examined scanning electron microscopy by a VEGA//TSCAN. In addition, Vicker's hardness of the samples was carried out by applying a hardness indenter with a load of 10 kgf.

* Corresponding author. Tel./fax: +98 2144435663.
E-mail address: nkhademian@gmail.com (N. Khademian).

0925-8388/$ - see front matter © 2012 Elsevier B.V. All rights reserved.
http://dx.doi.org/10.1016/j.jallcom.2012.08.035

3. Results and discussions

Fig. 1 shows a multiplot of XRD patterns of the as-cast 4 mm diameter $Zr_{65-x}Cu_{17.5}Ni_{10}Al_{7.5}V_x$ (x = 0, 1, 2, 3, 5 at.%) alloys. As shown in Fig. 1, for the sample without vanadium and the sample with x = 1; there are broad diffuse peaks between diffraction angles from 35° to 50° without detectable sharp diffraction peaks, indicating the glassy state of the samples. The increase of V concentration from 2 to 5% causes some diffraction peaks appear on the patterns corresponding to the precipitation of nanocrystalline phases. The size of them are about 20–50 nm according to the calculation by Scherer equation. The crystalline phases were indexed as the Zr_2Ni and Zr_2Cu phases in the as-cast rods.

Fig. 2 shows the DSC result of the as-cast $Zr_{65-x}Cu_{17.5}Ni_{10}Al_{7.5}V_x$ (x = 0, 1, 2, 3, 5) glassy alloys. During heating; the alloy exhibits distinct glass transition, followed by supercooled liquid region (SLR) and finally an exothermic peak corresponding to a crystallization reaction. The arrows, pointing down, indicate the glass transition temperature T_g and the onset crystallization temperature T_x. Fig. 3 indicates that the onset temperature of crystallization T_x and ΔT_x decrease; however, glass transition temperature increases with the increase of V content of the samples.

Therefore glass forming ability of $Zr_{65}Cu_{17.5}Ni_{10}Al_{7.5}$ BMG is deteriorated with partial addition of V because though, there is a considerable difference between atomic radius of Zr and V; there are not large atomic size differences among Cu, Al, Ni and V as shown in Table 1 [21]. On the other hand, it was proposed that the addition of V more than 1 at.% can destabilize the melt of $Zr_{65}Cu_{17.5}Ni_{10}Al_{7.5}$ alloy [13,17,19]. Therefore, the instability of the undercooled liquids leads to precipitation of nanocrystalline phases.

Fig. 4 shows the nominal compressive stress–strain curves of the as-cast $Zr_{65-x}Cu_{17.5}Ni_{10}Al_{7.5}V_x$ (x = 0, 1, 2, 3, 5) alloys. In uniaxial compression, $Zr_{65}Cu_{17.5}Ni_{10}Al_{7.5}$ bulk metallic glass exhibit fracture strength (σ_f) about 1400 MPa but no plasticity. As V content of samples increases from 0 to 1 at.%, the strength as well as plasticity increases a little. Further increase of V content, from 1 to 2 at.%, causes ultimate strength (σ_u), fracture strength and fracture strain to increase as indicated in the insert of Fig. 4. It is also shown that in the sample with x = 2 the ultimate strength of 1690 MPa, the fracture strength of 1674 MPa and fracture strain of 3% are the highest properties being reached among the samples. However, the increase of V content more than x = 2 (i.e. 3 and 5) decreases fracture strength and strain simultaneously. The results, in the right inset of Fig. 4, show an increase in the elastic moduli of samples with increasing V contents.

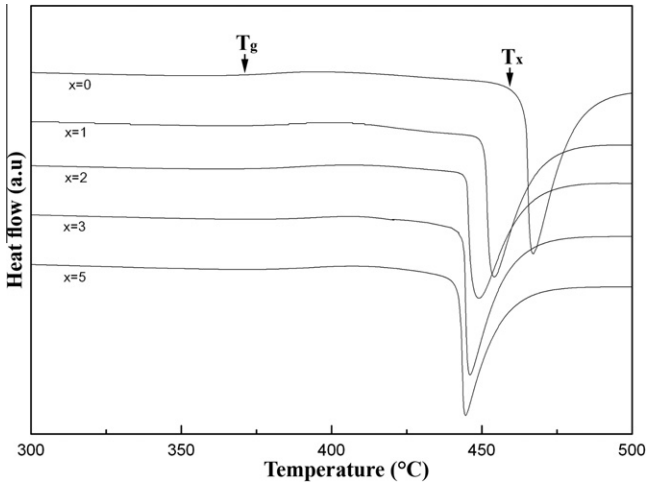

Fig. 2. DSC curves of as-cast $Zr_{65-x}Cu_{17.5}Ni_{10}Al_{7.5}V_x$ (x = 0, 1, 2, 3, 5) alloys at a heating rate of 20 K/min.

Fig. 5 shows the fracture surfaces of the as-cast $Zr_{65-x}Cu_{17.5}Ni_{10}Al_{7.5}V_x$ (x = 0, 1, 2, 3, 5) BMGs. The angle between the fracture surface and the compression axis for the samples with x = 0, 1, 2, 3 is close to 42°; however, there is a deviation of three degree at the end of the fracture as shown in Fig. 5a to Fig. 5d. In the sample with x = 5 there are intersecting fracture planes with different angles without any shear band as indicated in Fig. 5(e). On the other hand in the sample with x = 2 branching of shear bands has been occurred much more than that of in the other samples.

Fig. 6 exhibits the SEM micrographs of the fracture surface of the as-cast $Zr_{65-x}Cu_{17.5}Ni_{10}Al_{7.5}V_x$ (x = 1, 2, 3, 5) alloys. The vein patterns (VP) and semi-liquid regions (SLR) were observed on the

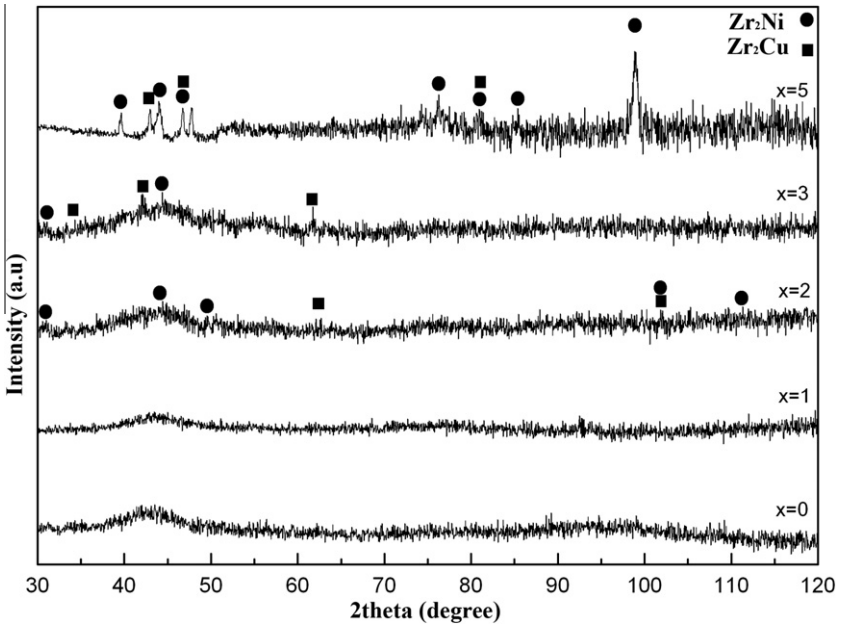

Fig. 1. X-ray diffraction patterns for the as-cast $Zr_{65-x}Cu_{17.5}Ni_{10}Al_{7.5}V_x$ (x = 0, 1, 2, 3, 5) alloys.

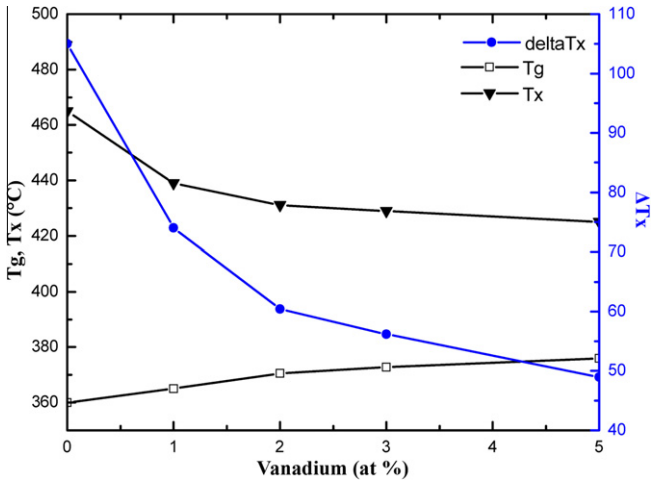

Fig. 3. Variations of supercooled liquid region (ΔT_x), transition temperature (T_g) and onset crystallization temperature (T_x) of as-cast $Zr_{65-x}Cu_{17.5}Ni_{10}Al_{7.5}V_x$ (x = 0, 1, 2, 3, 5) alloys.

Table 1
Atomic size differences among Zr, Cu, Al, Ni and V [23].

Atomic size differences (%)	
Zr–V	16.25
Cu–V	4.68
Ni–V	8.6
Al–V	6.29

fracture surface of the specimen with x = 1, as shown in Fig. 6(a). For the sample with x = 2, it shows river patterns (RP) with a few vein patterns as indicated in Fig. 6(b). On the other hand, Fig. 6(c) shows the typical fracture surface with river patterns (RP), shear bands (SB) and microcracks (MC); while Fig. 6(d) exhibits a cleavage-like morphology and microcracks (MC) on the fracture surface.

The present results demonstrate that small amount of V addition can have a considerable effect on mechanical properties of $Zr_{65}Cu_{17.5}Ni_{10}Al_{7.5}$ BMG. According to the results shown in Fig. 5(c) and Fig. 4 for $Zr_{63}Cu_{17.5}Ni_{10}Al_{7.5}V_2$ alloy give rise that plastic deformation is accommodated through the generation of multiple shear bands which is probably related to an excellent interfacial bonding between crystallites and amorphous matrix [22] leading to the shear bands cannot easily transform into cracks. The quenching causes the introduction of compressive residual stress field in amorphous phase because of the significant difference in the coefficients of thermal expansion between metallic glass matrix and crystalline phases [10]; therefore, the improved ductility is also considered to originate from the formation of multiple shear bands initiated at the interface of the nanocrystalline phases and amorphous matrix [1,16,23,24].

The critical resolved shear stress (τ) of the as-cast $Zr_{65-x}Cu_{17.5}Ni_{10}Al_{7.5}V_x$ alloys decreases with the increase of V content from 3 at.% as shown in Fig. 7. The critical resolved shear stress can be calculated from the normal stress on the shear plane by the following equation:

$$\tau = \sigma_0 \cos\varphi \cos\theta$$

where θ is the angle between shear plane and loading axis, and φ is the angle between the loading axis and normal stress (σ_n) direction as depicted in the inset of Fig. 7. The results provide the Boltzmann correlation between τ and V content. In fact, the addition of V changes the mechanical properties of Zr-based BMG and especially for alloy 5 at.%, i.e. we can see complex and different behavior from monolithic BMG, because multi-plane fracture surfaces for alloy 5 at.% has a completely wide range of critical resolved shear stress.

The Young's modulus (E) correlates with fracture theoretical strength (σ) of material as $\sigma = \sqrt{\frac{E\gamma}{d}}$ where γ is the surface energy per unit area, and d is the spacing of parallel atomic planes. For normal solids, σ is estimated to be about $E/10$. However, crystalline materials typically have fracture stresses are lower than the theoretical value (about $E/500$–$E/10000$) [25]. This leads to this conclusion that dislocations are responsible for the lower than ideal fracture strength of crystalline materials.

Primary analysis based on limited data from metallic glasses show a clear good correlation between fracture strength and Young's modulus ($E/\sigma \approx 50$), and hardness (Hv) and E ($E/Hv \approx 20$); and also the relation between Hv and σ for these glasses show a good correlation as $Hv = 2.5\sigma$. However, for these metallic

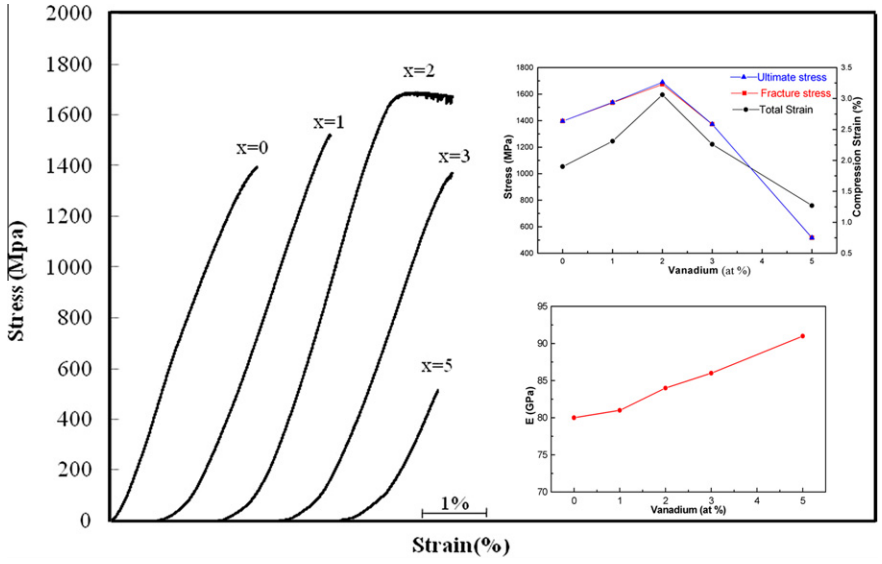

Fig. 4. Room temperature compression stress–strain plots of as-cast $Zr_{65-x}Cu_{17.5}Ni_{10}Al_{7.5}V_x$ (x = 0, 1, 2, 3, 5) alloys, and the right up inset is the parameters derived from the plots versus vanadium atomic percents, the right down inset show the elastic moduli for the as-cast $Zr_{65-x}Cu_{17.5}Ni_{10}Al_{7.5}V_x$ (x = 0, 1, 2, 3, 5) alloys.

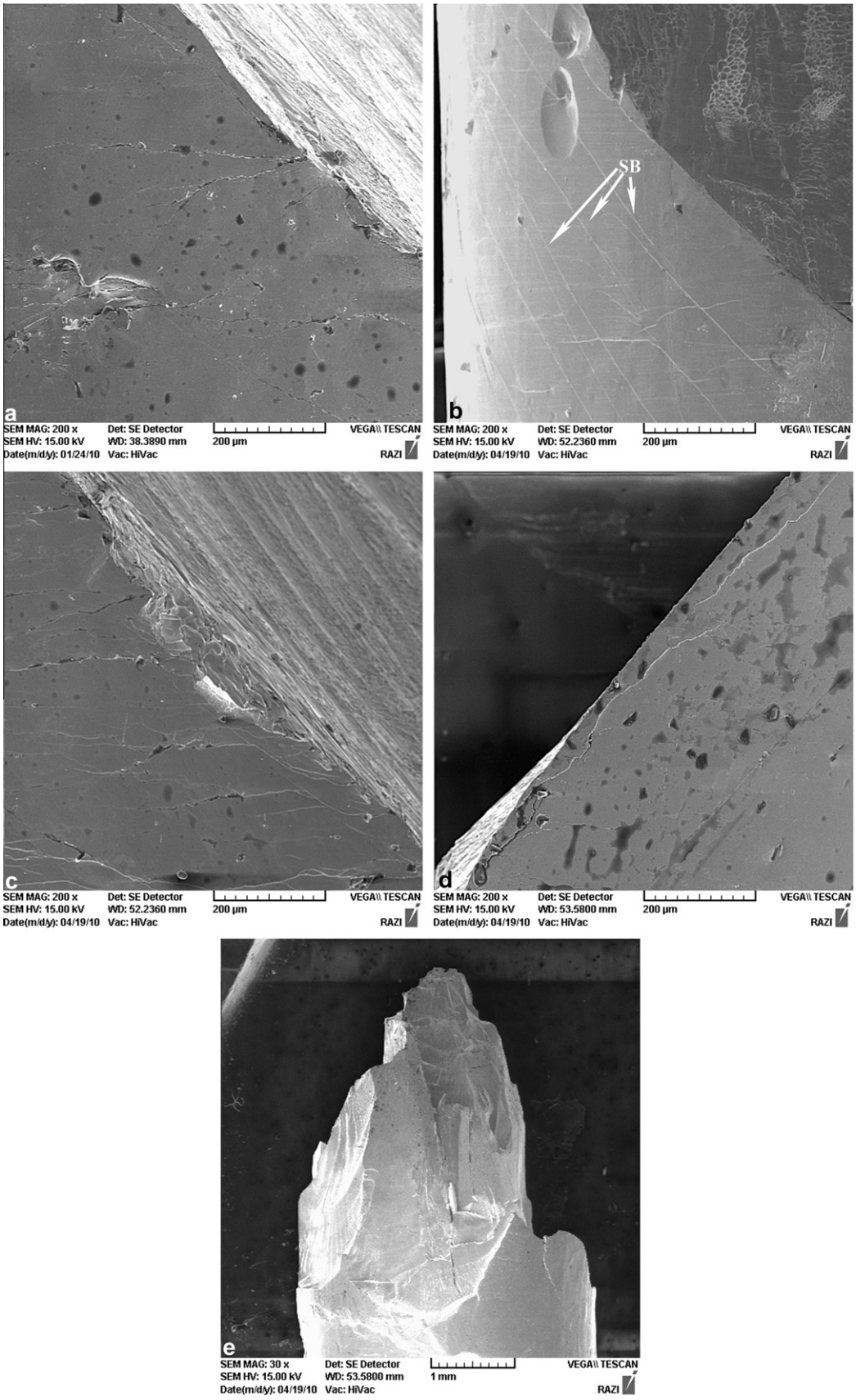

Fig. 5. Typical fractography features of as-cast $Zr_{65-x}Cu_{17.5}Ni_{10}Al_{7.5}V_x$ lateral surface of the sample with (a) $x = 0$, (b) $x = 1$, (c) $x = 2$, (d) $x = 3$, (e) $x = 5$.

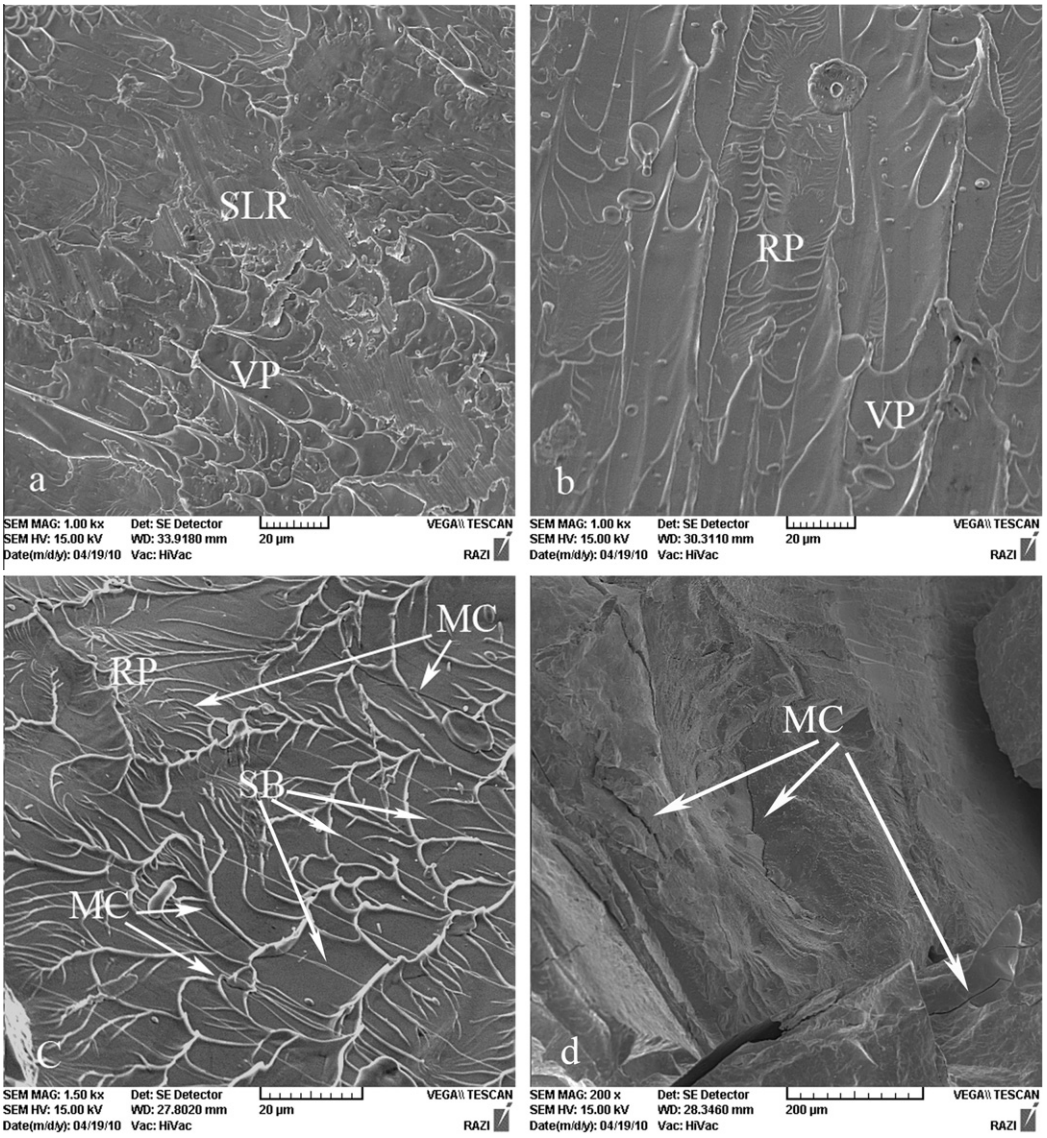

Fig. 6. Fracture surface features of as-cast $Zr_{65-x}Cu_{17.5}Ni_{10}Al_{7.5}V_x$ (a) $x = 1$ (b) $x = 2$ (c) $x = 3$ (d) $x = 5$.

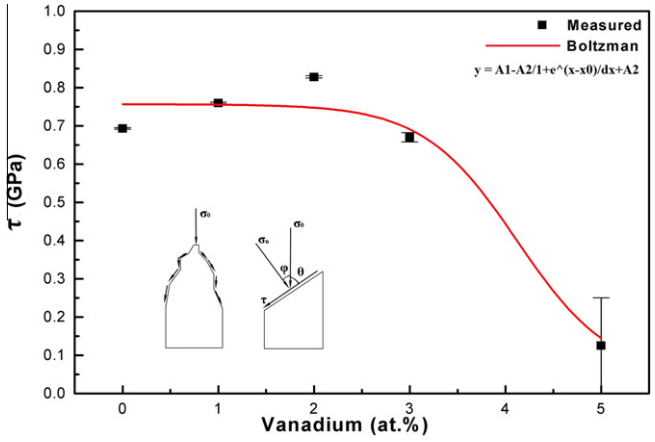

Fig. 7. The critical resolved shear stress (τ) of the as-cast $Zr_{65-x}Cu_{17.5}Ni_{10}Al_{7.5}V_x$ alloys.

glasses, E/σ *is 50*, which approximately 10–200 times larger than those of their crystalline materials and close to the theoretical strength ($E/10$). This indicates the fundamental mechanical properties of the bulk metallic glasses are significantly different from those of crystalline alloys. However, there is an empirical correlation between E of the metallic glasses and Tg ($Tg \propto 2.5\,E$), it is generally known that the Tg is dominated by the bonding force among the constituents, consequently, the high mechanical strength of the BMGs is due to stronger bonding force among the constituent elements [25]. Although, it is remarkable that the spread is so small for a lot of number of BMGs with respect to reference [25], the spread is noticeable when a comparison carried out among different groups of BMGs. We show these data on some metallic glasses plotted in Fig. 8(a–d) that the fit line put on the data of each group, they exhibit great deviation among parameters (E/σ, E/Hv, $Hv = 2.5\sigma$ and $Tg \propto 2.5\,E$). Therefore, the rough correlation between mentioned parameters is regarded to be a reflection of the difference in the deformation and fracture mechanism among the various bulk metallic glasses.

Fig. 9(a) shows a polynomial correlation between elastic moduli (E) and fracture strength (σ), i.e., fracture strength increases with increase of elastic moduli (up to 2 at.% V content) and then decreases with increase of elastic moduli in the higher V contents.

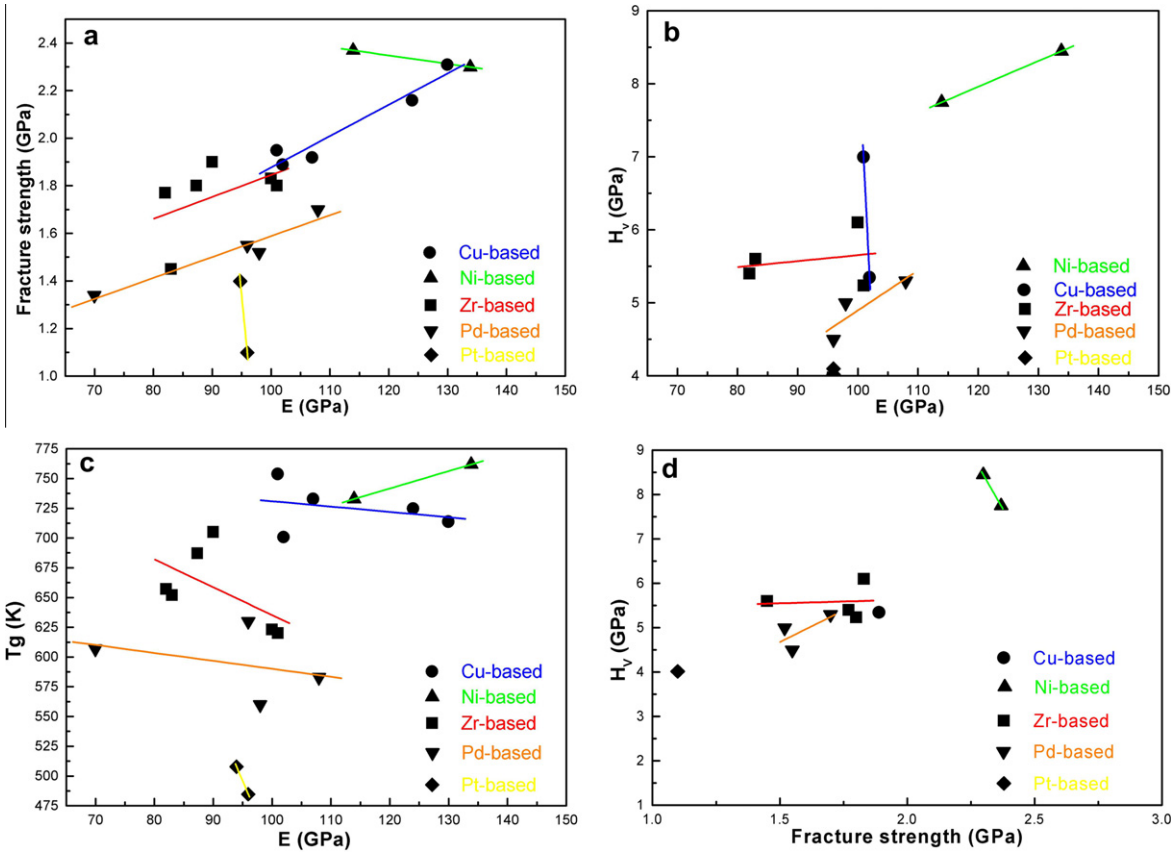

Fig. 8. (a) The correlation of fracture strength with elastic modulus, (b) the correlation of hardness with elastic modulus, (c) the correlation of glass transition temperature with elastic modulus, (d) the correlation of fracture strength with hardness; for the metallic glasses which are in Ref. [25].

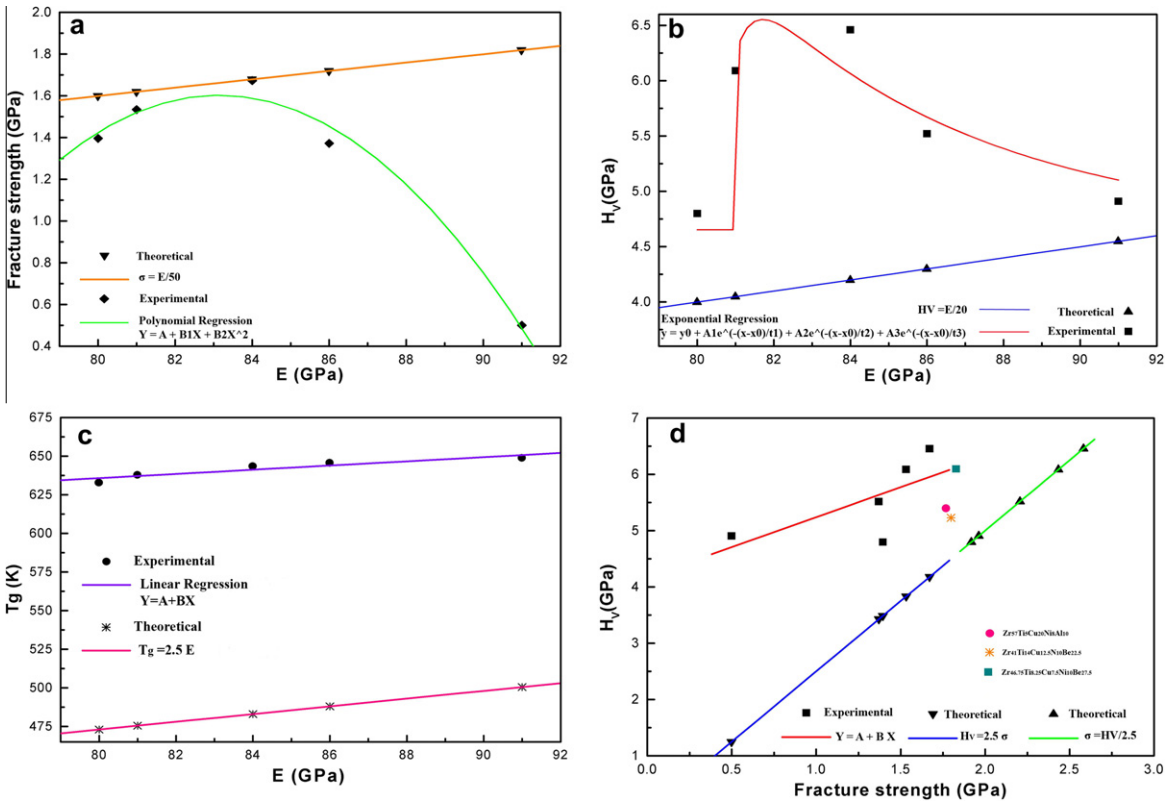

Fig. 9. (a) The correlation of fracture strength with elastic modulus, (b) the correlation of hardness with elastic modulus, (c) the correlation of glass transition temperature with elastic modulus, (d) the correlation of fracture strength with hardness; for the as-cast $Zr_{65-x}Cu_{17.5}Ni_{10}Al_{7.5}V_x$ (x = 0, 1, 2, 3, 5) alloys.

Fig. 9(b) shows an exponential correlation between elastic moduli and hardness (*Hv*), i.e., hardness increases with increase of elastic moduli (up to 2 at.% V content) and then decreases with increase of elastic moduli in the higher V contents.

In both of cases as mentioned above, there exists much deviation between measured quantities and theoretically anticipated quantities, because fracture mechanism with increase of V contents more than 2 at.% changes from shear bands to microcracks that is related to formation of nano crystallites which have weak interface or decrease of free volumes in metallic glass matrix [26]. BMGs exhibit isotropic elastic constants, but changing in short/middle range order structure [18] or formation of nanocrstalline could causes to non-isotropic elastic constants in samples, even dislocations may be accompanied [27] with shear bands into in situ bulk metallic glass composites. However, the detailed mechanism for the deformation and fracture needs to be further investigated.

Fig. 9(c) shows a linear correlation between elastic moduli and glass transition (*Tg*), i.e., *Tg* continually increases with increase of elastic moduli ($Tg \propto 1.35\,E$) or increase of V contents. Fig. 9(d) shows relatively good correlation between fracture strength and hardness, i.e., hardness increases with increase of fracture strength ($Hv \propto 1.06\sigma$).

The results suggest that the existence of the positive correlation does not only depend on the chemical composition of the metallic glasses but should be also related to the intrinsic homogeneous glassy structure. The high strength is intrinsic in BMGs and closely related to two parameters: (1) their elastic properties (2) structure of BMGs in nano or micro scale. At least, these correlations may assist in understanding the mechanisms of the plastic flow and fracture in metallic glassy systems.

4. Conclusion

(1) The addition of V is effective for a decrease in GFA of BMGs.
(2) $Zr_{63}Cu_{17.5}Ni_{10}Al_{7.5}V_2$. BMG exhibits a combination of high maximum strength of 1690 and total plastic strain of about 3%.
(3) The plasticity improved only when V was substituted for Zr in a limited composition range. Due to, shear band interaction with the crystalline phases, shear bands are multiplied and branched, and their rapid propagation is inhibited.
(4) The addition of V is strongly effective on the deformation and fracture mechanism of Zr-based BMGs. In fact, critical resolved shear stress (τ) of the $Zr_{65-x}Cu_{17.5}Ni_{10}Al_{7.5}V_x$ alloys decreases with the increase of V content.
(5) The correlations between the elastic modulus with fracture strength and Vicker's hardness are not linear, but the correlations between the elastic modulus and glass transition, and also between fracture strength and Vicker's hardness are linear for $Zr_{65-x}Cu_{17.5}Ni_{10}Al_{7.5}V_x$ ($x = 0, 1, 2, 3, 5$) bulk metallic glasses.

Acknowledgements

This work was financially supported by the research found of Materials Engineering and Manufacturing Technology Company (MEMT). The authors would like to acknowledge Mr. Mohammadi for their effective helps in this research.

References

[1] W.H. Wang, Prog. Mater Sci. 52 (2007) 540.
[2] A.Inoue, Mater. Sci. Eng. 304-306 (2001) 1.
[3] M.F. Ashby, A.L. Greer, Scripta Mater. 54 (2006) 321.
[4] W.H. Wang, C. Dong, C.H. Shek, Mater. Sci. Eng. 44 (2004) 45.
[5] W.H. Wang, Adv. Mater. 21 (2009) 4524.
[6] A.Inoue, X.M. Wang, W. Zhang, Rev. Adv. Mater. Sci. 18 (2008) 1.
[7] J.F. Loffler, Intermetallics 11 (2003) 529.
[8] J.F. Loffler, Int. J. Mat. Res. 97 (2006) 225.
[9] G. He, W. Loser, J. Eckert, Scripta Mater. 48 (2003) 1531.
[10] A. Inoue, T. Zhang, M.W. Chen, T. Sakurai, J. Saida, M. Matsushita, J. Mater. Res. 15 (2000) 2195.
[11] A. Gebert, J. Eckert, L. Schultz, Acta Mater. 46 (1998) 5475.
[12] J. Saida, M.S.E. Eskandarany, A. Inoue, Scripta Mater. 48 (2003) 1397.
[13] J.Saida, A. Inoue, J. Non-Cryst. Solids 312-314 (2002) 502.
[14] C. Fan, A. Inoue, Scripta Mater. 45 (2001) 115.
[15] I. Gallino, M.B. Shah, R. Busch, Acta Mater. 55 (2007) 1367.
[16] Y.F. Sun, C.H. Shek, B.C. Wei, W.H. Li, Y.R. Wang, J. Alloys Comp. 403 (2005) 239.
[17] L. Liu, K.C. Chan, M. Sun, Q. Chen, Mater. Sci. Eng. 445-446 (2007) 697–706.
[18] L. Liu, C.L. Qiu, M. Sun, Q. Chen, K.C. Chan, G.K.H. Pang, Mater. Sci. Eng. 449-451 (2007) 193–197.
[19] J. Saida, A. Inoue, Condensed Mater. 13 (2001) L73.
[20] H.R. Wang, Y.L. Gao, G.H. Min, Y.F.Ye, Y. Chen, Z.Q. Shi, X.Y.Teng, J. Alloys Comp. 349 (2003) 140.
[21] Avilable at: http://en.wikipedia.org/wiki/Atomic_radius
[22] J. Liu, H. Zhang, H. Fu, Z.Q. Hu, X. Yuan, J. Mater. Res. 25 (2010) 1159–1163.
[23] J. Lendvai, J. Gubicza, J.L. Labar, Z. Kuli, Int. J. Mat. Res. 100 (2009) 439.
[24] M. Kusy, U. Kuhn, A. Concustell, A. Gebert, J. Das, J. Eckert, L. Shultz, M.D. Baro, Intermetallics 14 (2006) 982.
[25] W.H. Wang, J. Non-Cryst. Solids 1481-1485 (2005) 351.
[26] F. Hori, T. Yano, Y. Yokoyama, Y. Akeno, T.J. Konno, J. Alloys Comp. 430-435 (2007) 207–210.
[27] F. Szuecs, C.P. Kim, W.L. Johnson, Acta Mater. 49 (2001) 1507–1513.